9 Stability Analysis: Practical Problems in Rock Slopes

A.B. Singh
Institute of Engineering, Tribhuvan University,
Pulchowk Campus, Lalitpur, Nepal

The first part of this paper attempts to assess rock mass qualitatively and as far as possible quantitatively in the light of recent developments in the field of rock mechanics. It also provides the basic theoretical background needed for the analysis of the most common types of rock slope failure. The second part discusses examples of the stability analysis of rock slopes at the dam sites of the Upper Arun and Kali Gandaki A hydroelectric projects in Nepal. The analyses are based on information provided by field geologists. The geological and geotechnical conditions in the Upper Arun were not complex so the stability analysis of the rock slopes at this site was more definitive. The geological and geotechnical conditions for the Kali Gandaki A Project were more difficult to interpret, for example the contact between dolomite and phyllites inside the slope could not be ascertained unequivocally even after the conclusion of the design phase. It is likely that problems will be encountered during construction at Kali Gandaki A.

Introduction

In certain situations, stability problems in rocks and soils may appear similar. However, there are a number of characteristics of rock mass that can lead to modes of slope failure that are quite different to those for soils. The first part of this paper deals with the stability problems related to rock or rock slopes, including the structural features related to stability, assessment of rock characteristics, and types of rock slope failure.

Rock or **rock mass**, invariably contains geological weakness planes such as joints, fractures, faults, bedding planes, and foliation planes. From the engineering point of view, rock or rock mass is the total in situ medium including all these discontinuities; **rock material, rock matrix,** or **intact rock** refers to the intact material between discontinuities, for example a hard piece of rock taken from a drill core.

Rock mass may contain various geological discontinuities oriented or distributed in various ways. It is the nature and distribution of these features within a rock mass that mainly governs its behaviour. The rock material is generally stronger than the rock mass and in most cases, except with soft sedimentary rocks, it is not the failure of intact rock but of weaker material and along planes of separation that leads to failure. However, failure will also pass through the intact material and hence, for the same type of rock structure, rock masses that contain stronger intact rock matrices are usually stronger.

It is important to emphasise that rock mass behaviour cannot be described easily in the way possible for materials such as concrete, steel, and some soils. Many variables govern the behaviour of rock masses. These usually vary so widely that scientists must often satisfy themselves with only approximate indications. The most important thing is to make as best an assessment as is possible. Very sophisticated patterns may be mapped out for a rock matrix but failure might take

place along a pre-existing geological discontinuity. This is where a competent engineer needs field experience coupled with a theoretical knowledge of the principles of rock mechanics in order to be able to make sound judgements. Furthermore, practicality demands that geological and rock mechanics data be interpreted in both physical and mechanical terms. Over the years, rock mechanics has made considerable progress and methods have been developed. For example, quantitative methods have now been developed to assess the mechanical behaviour of some geological discontinuities.

In what follows, an attempt will be made to summarise briefly the ways in which rock mass can be characterised and to give examples of how the knowledge so gained is used in practice.

Part A: Geotechnical Background For Rock Slope Analysis

Major Types of Structural Features

There are a number of excellent publications which describe the structural features of rock masses (Price 1966). The most common rock structures — bedding planes, folds, faults, joints, and, shear zones — are described below.

Bedding planes are characteristic of sedimentary rocks and serve to divide these kinds of rocks into a number of beds or strata. Bedding planes are usually very persistent particularly if their deposition has taken place in a wide-open sea in calm water conditions. However, if the sediments are laid down rapidly from heavily laden winds or water currents, bedding planes may have cross or discordant features. In each case bedding planes represent planes of weakness; these planes of weakness may be parallel to the bedding planes if there was no other preferred orientation of particles during deposition. Usually, the strength parameters of the bedding planes will have both cohesion and friction components, but they will be considerably smaller than those in an orthogonal direction.

Folds are formed when the orientation of beds is changed by flexing following the application of post-depositional tectonic forces. Folds range from major structures extending up to several kilometres long to very small localised features. During the folding process, shear stresses are set up between the beds which may reduce the bedding plane shear strength. Large-scale folds, when considered on a regional scale, may be thought of as a rough excrescence which increases the shear strength due to increased frictional resistance. The prominent features generally associated with folds are well-defined sets of joints that are formed in the crest, trough, and limbs of the fold and which divide the rock into discrete elements (Figure 9.1). The higher the number of discontinuities associated with folding, the weaker a rock mass will be. Further information can be found in Price (1966).

Faults are basically fractures on which relative displacement has taken place on opposite sides of a fault plane due to shear. Faults may be pervasive and may extend to several hundred kilometres long, as with the 1,500 km long San Andreas Fault in California, USA. On the other hand they may be of local extent and only metres or centimetres long. The fault zone thickness can also vary from millimetres in the case of local faults to metres and even hundreds of metres in the case of regional faults. A fault zone may contain weak material such as fault gouge (clay), fault breccia (cemented angular rock fragments), rock flour, or granular material. The walls may be coated with minerals such as graphite and chlorite and as a result will have low shear strength. In addition, the fault zone or the area adjacent to the fault may be crushed and disturbed by drag folds or secondary faults or

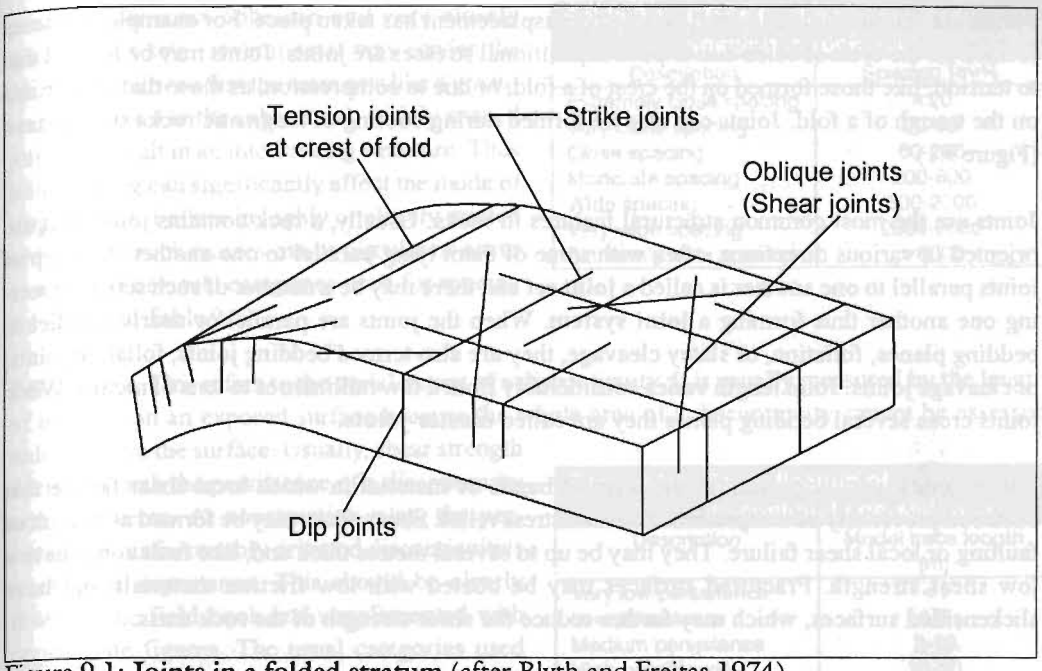

Figure 9.1: **Joints in a folded stratum** (after Blyth and Freitas 1974)

joints (Figure 9.2). The combined effect of all these factors is to reduce the shear strength of the fault zone and increase the instability of the rock containing the fault.

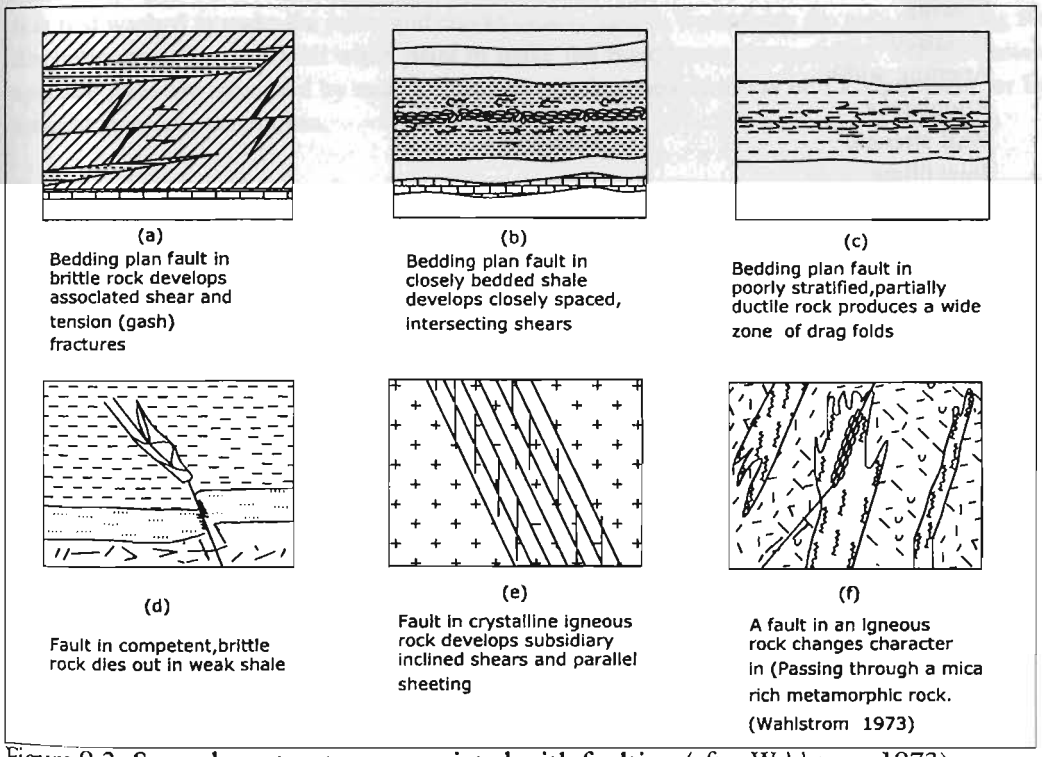

Figure 9.2: **Secondary structures associated with faulting** (after Wahlstrom 1973)

Joints are fractures along which no relative displacement has taken place. For example, fractures formed on the crest of folds due to post-depositional stresses are joints. Joints may be formed due to tension, like those formed on the crest of a fold, or due to compression, as those that are formed on the trough of a fold. Joints can also be formed during cooling of magmatic rocks such as lava (Figure 9.1).

Joints are the most common structural features in rocks. Usually, a rock contains joints that are oriented in various directions, often with some of them lying parallel to one another. A group of joints parallel to one another is called a **joint set** and there may be a number of such sets intersecting one another thus forming a **joint system**. When the joints are parallel or nearly parallel to bedding planes, foliation, or slatey cleavage, they are also termed bedding joints, foliation joints, or cleavage joints. Joint length varies considerably from a few millimetres to tens of metres. When joints cross several bedding planes they are called **master joints**.

Shear zones usually present in the form of bands of material in which local shear failure that occurred previously now represents zones of stress relief. Shear zones may be formed as a result of faulting or local shear failure. They may be up to several metres thick and, like fault zones have a low shear strength. Fractured surfaces may be coated with low friction materials and have slickensided surfaces, which may further reduce the shear strength of the rock mass.

Rock Mass Characterisation

In order to assess the in situ behaviour of rock mass, the following parameters related to geological discontinuities and rock structure should be investigated and mapped in the field.

- Orientation
- Spacing
- Persistence
- Aperture width
- Roughness
- Wall strength
- Joint filling
- Seepage conditions
- Joint set number
- Block size

Orientation – The orientation of a discontinuity denotes its three-dimensional position in space and is described by the dip direction (the direction perpendicular to the strike of the rock strata) and dip amount or inclination (the angle it makes with a horizontal plane, measured in the dip direction). The orientation of discontinuities relative to an engineering structure has an extremely important effect on the stability of that structure. For example, a rock bed dipping with a slope increases the instability of the slope, while one dipping into the slope may increase stability. The importance of the orientation of a discontinuity increases when other conditions are present that can lead to deformation and instability. For example, weathering along the bedding plane will render slopes more unstable, if this is coupled with weathering along another set of joints the slope will be even more unstable. Water seepage usually adds to slope instability.

Spacing usually refers to the mean distance between adjacent discontinuities measured in a direction perpendicular to them. In general, it is also related to rock mass qualities such as cohesion and shear strength which increase with the increase in spacing. Closely spaced joint sets tend to

produce low mass cohesion and very closely spaced joint sets (several sets) may render the cohesion so low so that the mass acts like a granular soil mass. On the other hand, widely spaced joint sets result in an interlocking structure. Thus joint spacing can significantly affect the mode of slope failure. Failure in highly or closely jointed or fractured rock masses can be circular or occur as a flow. The usual categories used for spacing are shown in Table 9.1.

Table 9.1: Classification of discontinuity spacing in rock masses

Description	Spacing (mm)
Extremely close spacing	<20
Very close spacing	20-60
Close spacing	60-200
Moderate spacing	200-600
Wide spacing	600-2000
Very wide spacing	2000-6000
Extremely wide spacing	>6000

Persistence. This refers to the aerial extent of a discontinuity. It is usually measured by the length of its trace on an exposed surface because the whole area of a discontinuity cannot be assessed unless it is on the surface. Usually, shear strength decreases with the persistence of a discontinuity and vice versa. At construction sites, the persistence of unfavourably oriented discontinuities is of great importance. This should be clearly noted in the field book and supplemented with appropriate figures. The usual categories used for levels of persistence are shown in Table 9.2.

Table 9.2: Classification of discontinuity persistence

Description	Model trace length (m)
Very low persistence	<1
Low persistence	1-3
Medium persistence	3-10
High persistence	10-20
Very high persistence	>20

Aperture – The aperture is the perpendicular distance between adjacent rock walls filled either by air or water. Aperture sizes are measured using measuring tapes calibrated in mm. If the exposed surface containing the discontinuity trace is dirty, it is first washed to make the joints and cracks clearly visible. Sometimes the area containing the discontinuity is sprayed with white paint to make the finer traces more visible. For boreholes, aperture sizes are measured by means of periscopes, borehole cameras or TV equipment, or by integral sampling techniques.

Roughness is caused by surface irregularities and can consist of small-scale surface roughness or larger scale roughness, which is expressed by waviness. In the latter case, individual parts of the 'waves' may themselves be characterised by surface roughness. The higher the level of roughness, the higher the shear strength. Roughness is described in qualitative terms (Table 9.3).

Table 9.3: Classification of discontinuity roughness

Class	Description
I	Rough or irregular and stepped
II	Smooth and stepped
III	Slickensided and stepped
IV	Rough or irregular and undulating
V	Smooth and undulating
VI	Slickensided and undulating
VII	Rough or irregular and planar
VIII	Smooth and planar
IX	Slickensided and planar

Since roughness is associated with the angle of internal friction, it directly affects the shear strength of rock. Barton (1973) has carried out extensive model test studies to evaluate the effect of joint roughness on shear strength. He divided roughness into a number of qualitative categories such as stepped, undulating, and planar and suggested how to calculate the shear strength of rock by increasing the angle of internal friction due to roughness as follows.

$$\tau' = \sigma'_n \tan (\Phi' + I)$$

where

τ' is the shear strength (peak or residual),
Φ' the angle of friction (peak or residual),
σ'_n the normal stress, and
I the roughness angle or waviness.

Wall strength. Wall strength is an assessment of the compressive strength of adjacent rock walls. It is an important parameter of rock shear strength but may be considerably reduced due to weathering or alteration of the walls. However, if the rock walls are not in contact, the shear strength of the filling material may play the governing role.

Wall strength very much depends on whether adjacent walls are weathered or not. The degree of weathering is assessed following the well-known weathering classification scheme, which divides rock into 6 grades ranging from fresh rock to residual soil. Wall strength is usually determined either by manual index tests such, as the uniaxial compression test, or by the Schmidt hammer test.

Filling material – Filling material may change the shear strength of a rock mass considerably. The filling material may consist of sand, silt, clay, or breccia and include the thin coating material. When the filling material is thick, the design shear strength will be reduced to that of the filling material. In this case, the mineralogy, grading, over consolidation ratio (OCR), and moisture content of the filling material are also determined. When required, sampling needs to be done very carefully.

Seepage – Water may percolate through a discontinuity and may have free-flow conditions or it may just be free moisture. Free-flow conditions not only reduce the shear strength of rocks but often cause difficulties on construction sites. The seepage of water into rock masses and joints may keep filling material moist or it may seep out along the dip of the planes. However, water flow can also be large and wash out the filling material. It then becomes a serious problem particularly in tunnelling work as recently happened at Khimti Khola Hydel Project in eastern Nepal.

Number of Joint Sets – Joints that lie approximately parallel to one another constitute a joint set. The higher the number of such joint sets intersecting each other, the lower will be the shear strength.

Block Size – Block size refers to the dimensions of the individual rock blocks and pieces which result from the mutual orientation of intersecting joint sets as well as from the spacing of individual sets. Large block sizes usually indicate better interlocking; as the block size goes down, the rock mass tends to become more like a granular mass.

Geological Data Collection

Ultimately the above-mentioned parameters will have to be evaluated for a specific project site. In order that the geological data collected represent the site in question as reliably as possible, measurements should be done with a full knowledge of the scope and limits of geological field investigation and data collection. The extent of field investigations and the type of geological data to be collected depend on the scope of the particular project. However, whatever the scope of a study it is always good practice to start by reviewing the available information on regional geology. For example, stereoscopic examination of pairs of aerial photographs can reveal linear surface features that indicate underlying geological structures such as faults.

Field mapping, or structural data collection, involves investigating all of the ten parameters listed above in the area related to the project area. Mapping of the exposed rock outcrops and other

geological features is usually sufficient to analyse rock slope stability. Geological compasses and hammers and measuring tapes are usually required. What is most important in collecting data is that it should be representative and sufficient. Clearly it is not possible to map every point in a project area so the area must be sampled. The experience and judgement of the field geologist will indicate to him or her which portion of the rock mass should be sampled to obtain satisfactory results. Sampling is carried out either by line sampling or area sampling.

Line sampling involves stretching a long measuring tape along the face of an outcrop or excavation and recording every structural feature that intersects the tape. In **area sampling** the area is divided into an appropriately sized grid and all the structural features inside the selected grids are recorded. It is often difficult to assess the number of field measurements needed to represent a project area adequately. The suggested number of field measurements ranges from 300 to 2000 for a single site depending on the site conditions and the priorities.

One of the most important points related to field mapping is to ensure uniform data entry. The dates, times, location, and sketches of the discontinuities must be entered every day in the data book. Field geologists should not rely on their memories to record details later on.

Types of Rock Slope Failure

Rock slopes usually fail as a result of the presence of structural weaknesses such as weakness planes. Sometimes, one set of weakness planes may play the dominant role leading to plane failure, while in another case failures may be induced by two joint sets leading to wedge failure. When a rock mass is intensively fractured so that it is more like an assemblage of coarse-grained material its behaviour is more like that of a soil slope and the slope may fail in a circular fashion. Rock slope failures can be categorised as one of the following.

- Plane failure
- Wedge failure
- Circular failure
- Toppling failure
- Rock falls

In reality, particularly where failure involves a large volume of material, rock slope failure is more likely to be a combination of these types. The mechanics of different types of failure is described in considerable detail in Hoek and Bray 1981. In the following, a brief description is given of the most important points related to plane failure and wedge failure, the only two modes that can be treated with some mathematical accuracy.

Plane Failure

Plane failure usually takes place in rock slopes composed of sedimentary or stratified rocks when the strata dips towards the slope and the daylight in the slope. Plane failure comprises sliding on a single plane and is effectively two-dimensional; in many ways it can be considered as a special case of the more common, three-dimensional, wedge mode of failure. In practice plane failure is relatively rare in rock slopes, as it is rare for all the necessary geometrical conditions to be met. However, many valuable lessons can be learnt from a consideration of the mechanics of this simple mode of failure. In general, the geometrical conditions shown in Figures 9.3 a, b, c, and d and listed below are necessary for plane failure to occur.

- The plane on which sliding occurs must strike parallel or nearly parallel (within approximately $\pm 20^{0}$) to the slope face.

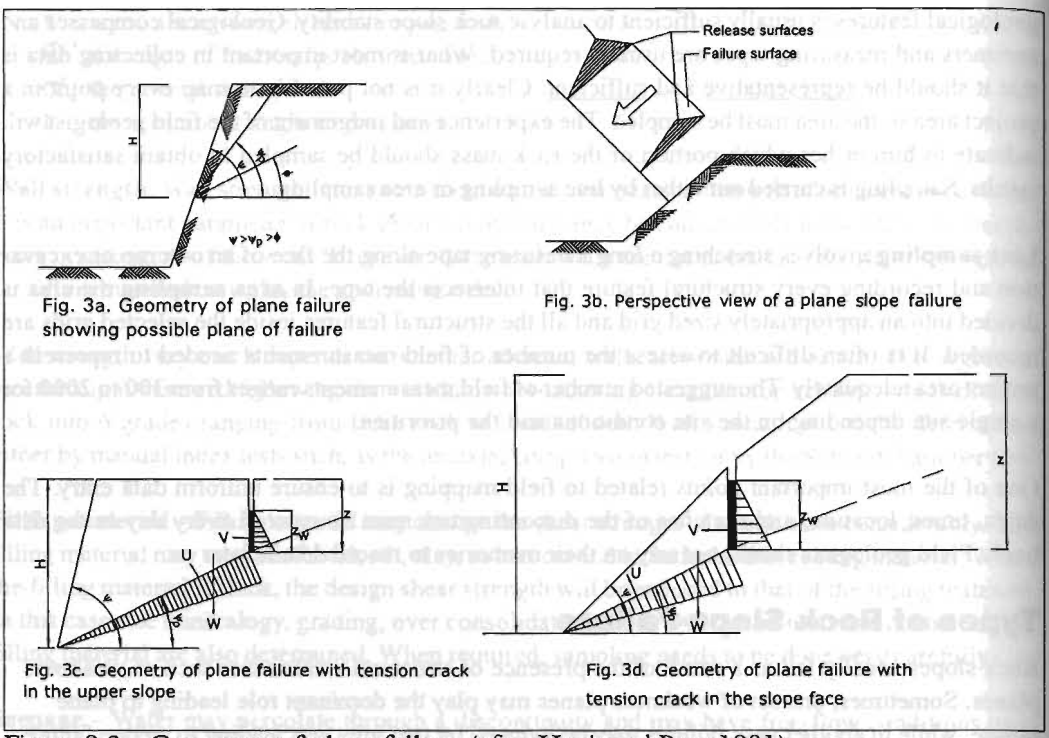

Fig. 3a. Geometry of plane failure showing possible plane of failure

Fig. 3b. Perspective view of a plane slope failure

Fig. 3c. Geometry of plane failure with tension crack in the upper slope

Fig. 3d. Geometry of plane failure with tension crack in the slope face

Figure 9.3: **Geometry of plane failure** (after Hoek and Bray 1981)

- The failure plane must 'daylight' on the slope. In other words its dip (Ψ_p) must be smaller than the dip of the slope face so that $\Psi > \Psi_p$, and the trace of the failure plane with the slope must be above the toe of the slope.
- The dip of the failure plane must be greater than the angle of friction (ϕ) of this plane so that $\Psi_p > \phi$
- The release surfaces on either side of the failed mass must provide negligible resistance to sliding.

Plane failures happen in two dimensions and so for the sake of analysis a slice measured in the direction perpendicular to the dip direction is usually taken. Once the dip angles corresponding to the slope and the failure surface are known, the surface area on which failure takes place as well as the volume of rock involved in the downward movement can be calculated easily. These parameters will, however, also depend on the geometry of the tension crack that may exist either on the slope itself or on its upper surface. Water may have access into the tension crack; the hydrostatic pressure will vary depending on whether the tension crack is dry or contains water.

Barton (1997) carried out very detailed studies on the failure of jointed rock slopes and concluded that tension cracks are formed as a result of very small shear movements within the rock mass. Hence, when a tension crack becomes visible on the surface it means that shear failure may well have started within the rock mass. It is therefore reasonable to assess the stability of a slope based on the condition of its limit state equilibrium.

Cohesion and friction parameters are either assumed, estimated, or calculated from field and/or laboratory tests or back calculations based on actual slope failures. In fact, the importance of the

field investigation and rock mass characterisation mentioned earlier lies exactly in assessing cohesion, friction angle, shear strength, and other design parameters. Once a reasonable assessment of these parameters has been made, the analysis becomes a simple matter of solving the following equation for the safety factor F, the ratio of the total force resisting sliding to the total force tending to induce sliding.

$$F = \frac{cA + (W\cos\psi_p - U - V\sin\psi_p)\tan\phi}{(W\sin\psi_p + V\cos\psi_p)} \quad (1)$$

Further

$$A = (H-z)\,\mathrm{cosec}\psi_p \quad (2)$$

$$U = \tfrac{1}{2}\gamma_w z_w (H-z)\,\mathrm{cosec}\psi_p \quad (3)$$

$$V = \tfrac{1}{2}\gamma_w z^2_w \quad (4)$$

and for a tension crack in the upper surface

$$W = \frac{1}{2}\gamma H^2\left[\left\{1-\left(\frac{z}{H}\right)^2\right\}\cot\psi_p - \cot\psi_f\right] \quad (5)$$

and for a tension crack in the slope face

$$W = \frac{1}{2}\gamma H^2\left\{\left(1-\frac{z}{H}\right)^2 \cot\psi_p(\cot\psi_p \tan\psi_f - 1)\right\} \quad (6)$$

where z is the depth of the tension crack measured from the top of the slope, z_w is the depth of water in the crack, W is the weight of the sliding block, U is the uplift force due to water pressure on the sliding surface, V is the force due to water pressure in the crack, c the cohesion, and ϕ the friction angle define the shear strength of the sliding surface, and ψ and ψ_p are the angles of dip of the slope face and the fault plane as shown in Figure 10.3.

Transformation from the first case (tension crack in the upper surface) to the second case (tension crack in the slope) occurs when the tension crack coincides with the crest so that:

$$z/H = (1-\cot\psi.\tan\psi_p) \quad (7)$$

Hoek and Bray (1981) have presented the same relationship in a more versatile form, which can accommodate a range of slope geometry, water depths, and variation in shear strength parameters. This is very useful for comparative analysis. The dimensionless relationship has the following form:

$$F = \left[\frac{2c}{\gamma H}p + \{Q\cot\psi_p - R(P+S)\}\tan\varphi\right] \Big/ \{Q + R.S\cot\psi_p\} \quad (8)$$

where,

$$P = (1-z/H)\,\mathrm{cosec}\psi_p \quad (9)$$

$$Q = [\{1-(z/H)^2\}\cot\psi_p - \cot\psi_f]\sin\psi_p \quad (10)$$

when the tension crack is in the upper surface

$$Q = [(1-z/H)^2\cos\psi_p(\cot\psi_p\tan\psi_f - 1)] \quad (11)$$

when the tension crack is in the slope face

$$R = (\gamma_w/\gamma).(z_w/z).(z/H) \quad (12)$$

$$S = (z_w/z).(z/H)\sin\psi_p \quad (13)$$

The ratios P, Q, R, and S are all dimensionless and depend on the geometry of the slope but not on its size. Note, however, that the depth of the tension crack z is always measured from the top of the slope. Hoek and Bray (1981) have presented the ratios P, Q, R, and S in graphical form for a range of slope geometries and these can be used directly to analyse the stability of rock slopes that are likely to fail by plane failure.

Depth and position of the critical tension crack

The analysis presented above assumes that all the parameters needed to calculate the safety factor F are known. In particular it assumes that the position of the tension crack is known from its visible trace and that its depth can be established by constructing an accurate cross-section of the slope. However, sometimes it becomes necessary to estimate some of the figures; for example, the tension crack may not be visible due to thick growth or other masking effects. As the influence of a tension crack on the safety factor is considerable, particularly when filled with water, it is necessary to estimate the most probable position of the tension crack and the critical tension crack depth. This will vary depending on the extent to which the crack is filled with water.

When the slope is dry or measures are taken to drain the slope, the water forces U and V are zero and equation (1) becomes

$$F = \frac{cA}{W\sin\psi_p} + \cot\psi_p \tan\phi \quad (14)$$

The critical tension crack depth z_c for a dry slope can be derived by partial differentiation of this equation with respect to z/H and equating the result to zero which gives:

$$z_c/H = 1 - (\cot\psi_f \tan\psi_p)^{1/2} \quad (15)$$

The corresponding position of the crack is

$$b_c/H = (\cot\psi \cot\psi_p)^{1/2} - \cot\psi_f \quad (16)$$

Similar calculations can be made for conditions when the crack is not dry or is filled with water to various heights. The safety factor starts to go down once a crack is filled to more than approximately one quarter of its depth, and reaches a minimum when the crack is water-filled. The minimum factor of safety is given by a water-filled tension crack that coincides with the crest of the slope, i.e., b = 0. An example of the effect of tension crack depth and the depth of water in it on the safety factor is given in Figure 9.4 (Hoek and Bray 1981).

Estimation of critical failure plane inclination

Slopes are more likely to fail where there is a well-defined failure plane such as with a through-going discontinuity surface. However, in many cases this does not exist and the failure surface can only be determined by minor geological features. This might be the case where the rock is highly fractured or when the discontinuity density is high.

Usually with soft rock slopes or soil slopes that have rather flat surfaces ($\psi < 45°$), the failure surface is circular, whereas in steep slopes the failure surface is nearly planar. The angle of inclina-

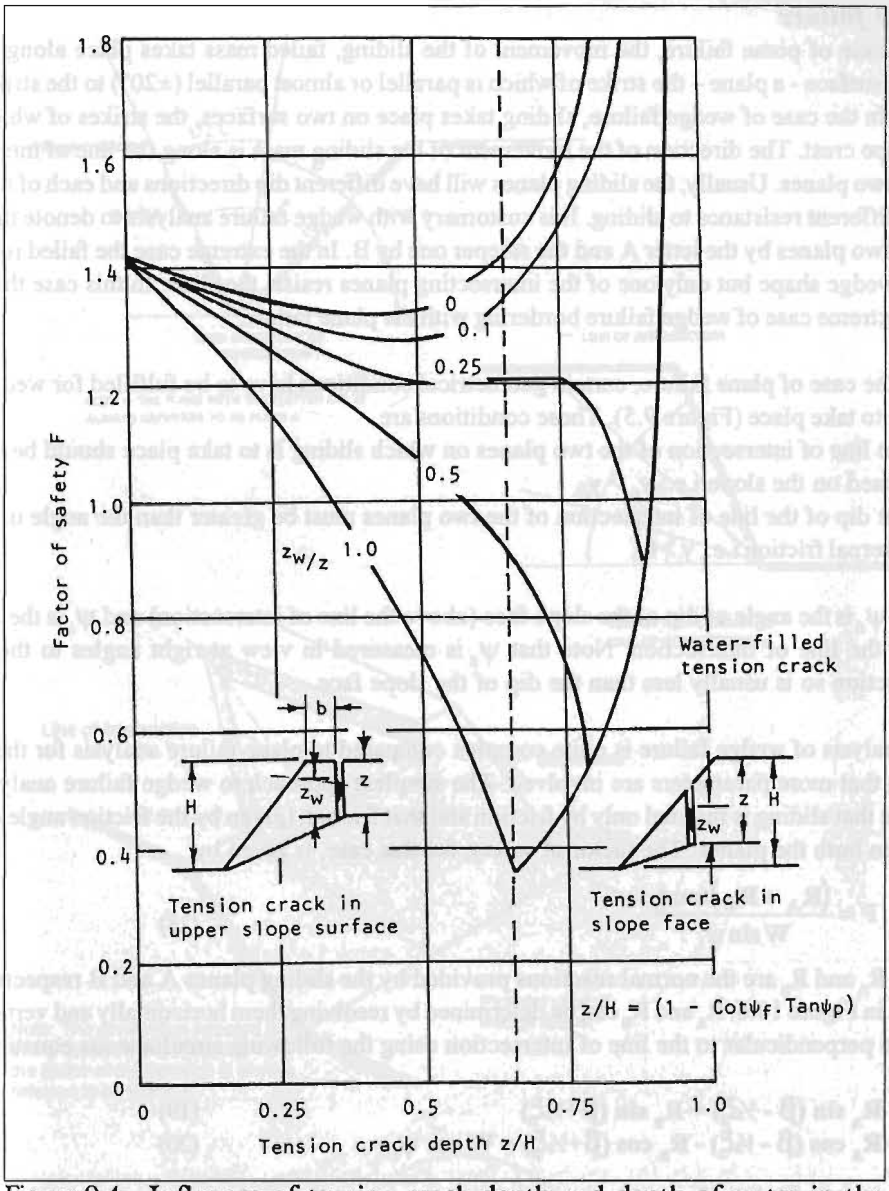

Figure 9.4: **Influence of tension crack depth and depth of water in the tension crack upon the safety factor of a typical slope (Hoek and Bray 1981)**

tion of the slope can be estimated by differentiating equation (1) with respect to ψ_p and equating the differential to zero. For dry slopes this gives a critical failure plane inclination ψ_{pc} of

$$\psi_{pc} = \tfrac{1}{2}(\psi + \phi) \qquad (17)$$

Hoek and Bray (1981) mention that the presence of water in cracks may reduce the failure plane inclination by about 10%. But they recommended the use of the above relationship for wet slopes on the grounds that this type of estimation is approximate and it is not justified to include the added complication of the influence of groundwater.

Wedge failure

In the case of plane failure, the movement of the sliding, failed mass takes place along a single failure surface - a plane – the strike of which is parallel or almost parallel (±20°) to the strike of the slope. In the case of wedge failure, sliding takes place on two surfaces, the strikes of which cross the slope crest. The direction of the movement of the sliding mass is along the line of intersection of the two planes. Usually, the sliding planes will have different dip directions and each of them will offer different resistance to sliding. It is customary with wedge failure analysis to denote the flatter of the two planes by the letter A and the steeper one by B. In the extreme case the failed rock mass has a wedge shape but only one of the intersecting planes resists the slide. In this case the failure is an extreme case of wedge failure bordering with the plane failure.

As in the case of plane failure, certain geometrical conditions have to be fulfilled for wedge failure to take place (Figure 9.5). These conditions are

- the line of intersection of the two planes on which sliding is to take place should be exposed on the slope i.e., $y_{fi} > y_i$
- the dip of the line of intersection of the two planes must be greater than the angle of internal friction i.e., $y_i > f$

where ψ_{fi} is the angle of dip of the slope face (above the line of intersection) and ψ_i is the angle of dip of the line of intersection. Note that ψ_{fi} is measured in view at right angles to the line of intersection so is usually less than the dip of the slope face.

The analysis of wedge failure is quite complex compared to plane failure analysis for the simple reason that more parameters are involved. The simplest approach to wedge failure analysis is to assume that sliding is resisted only by friction and that friction (given by the friction angle ϕ) is the same on both the planes. The factor of safety, for this case, is given by:

$$F = \frac{(R_A + R_B)\tan\phi}{W \sin\psi_i} \qquad (18)$$

where R_A and R_B are the normal reactions provided by the sliding planes A and B respectively as shown in Figure 10.6. R_A and R_B can be determined by resolving them horizontally and vertically on a plane perpendicular to the line of intersection using the following simultaneous equations.

$$R_A \sin(\beta - \tfrac{1}{2}\xi) = R_B \sin(\beta + \tfrac{1}{2}\xi) \qquad (19)$$

$$R_A \cos(\beta - \tfrac{1}{2}\xi) - R_B \cos(\beta + \tfrac{1}{2}\xi) = W \cos\psi_i \qquad (20)$$

where ξ is the included angle of the wedge and β the angle of tilt of the wedge (Figure 10.5).

Solving these equations and adding the values of R_A and R_B gives

$$R_A + R_B = \frac{W \cos\psi_i \sin\beta}{\sin\tfrac{1}{2}\xi} \qquad (21)$$

hence

$$F = \frac{\sin\beta}{\sin\tfrac{1}{2}\xi} \frac{\tan\phi}{\tan\psi_i} \qquad (22)$$

When only friction is considered, $(\tan\phi/\tan\psi_i)$ is the factor of safety for plane failure. Hence the above equation can be expressed as follows

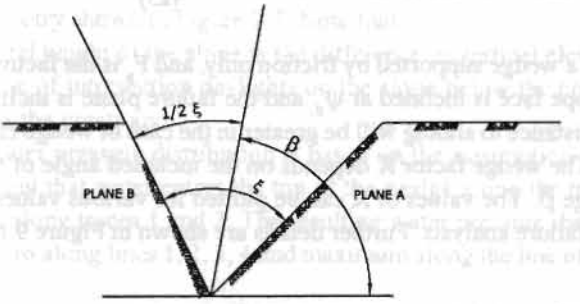

VIEW ALONG LINE OF INTERSECTION

NOTE :- THE PLANE WITH THE FLATTER DIP IS ALWAYS REFERRED TO AS PLANE A

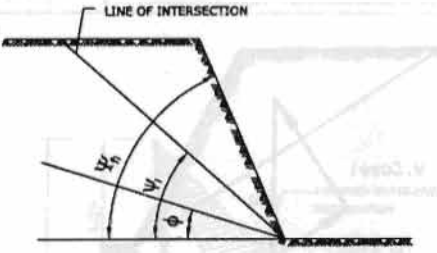

VIEW AT RIGHT ANGLES TO LINE OF INTERSECTION

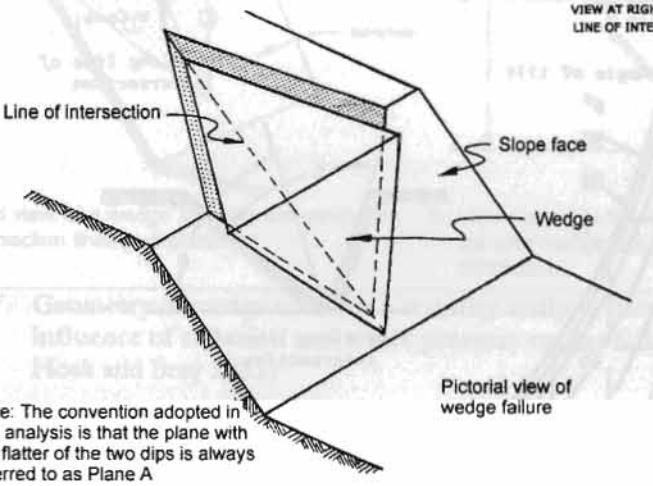

Pictorial view of wedge failure

Note: The convention adopted in this analysis is that the plane with the flatter of the two dips is always referred to as Plane A

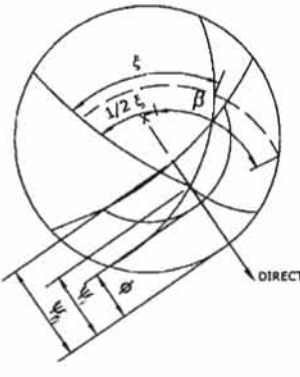

STEREOPLOT OF WEDGE FAILURE GEOMETRY

DIRECTION OF SLIDING

Figure 9.5: **Wedge failure geometry replaces former**

$$F_w = K F_p \qquad (23)$$

where F_w is the factor of safety of a wedge supported by friction only, and F_p is the factor of safety of a plane failure in which the slope face is inclined at ψ_f, and the failure plane is inclined at ψ_i. Since $K = (\sin\beta/\sin 0.5\xi) > I$, resistance to sliding will be greater in the case of wedge failure than that in the case of plane failure. The wedge factor K depends on the included angle of the wedge ξ and the angle of tilt of the wedge β. The values of K can be plotted for various values of ξ and β and be readily used for wedge failure analysis. Further details are shown in Figure 9.6.

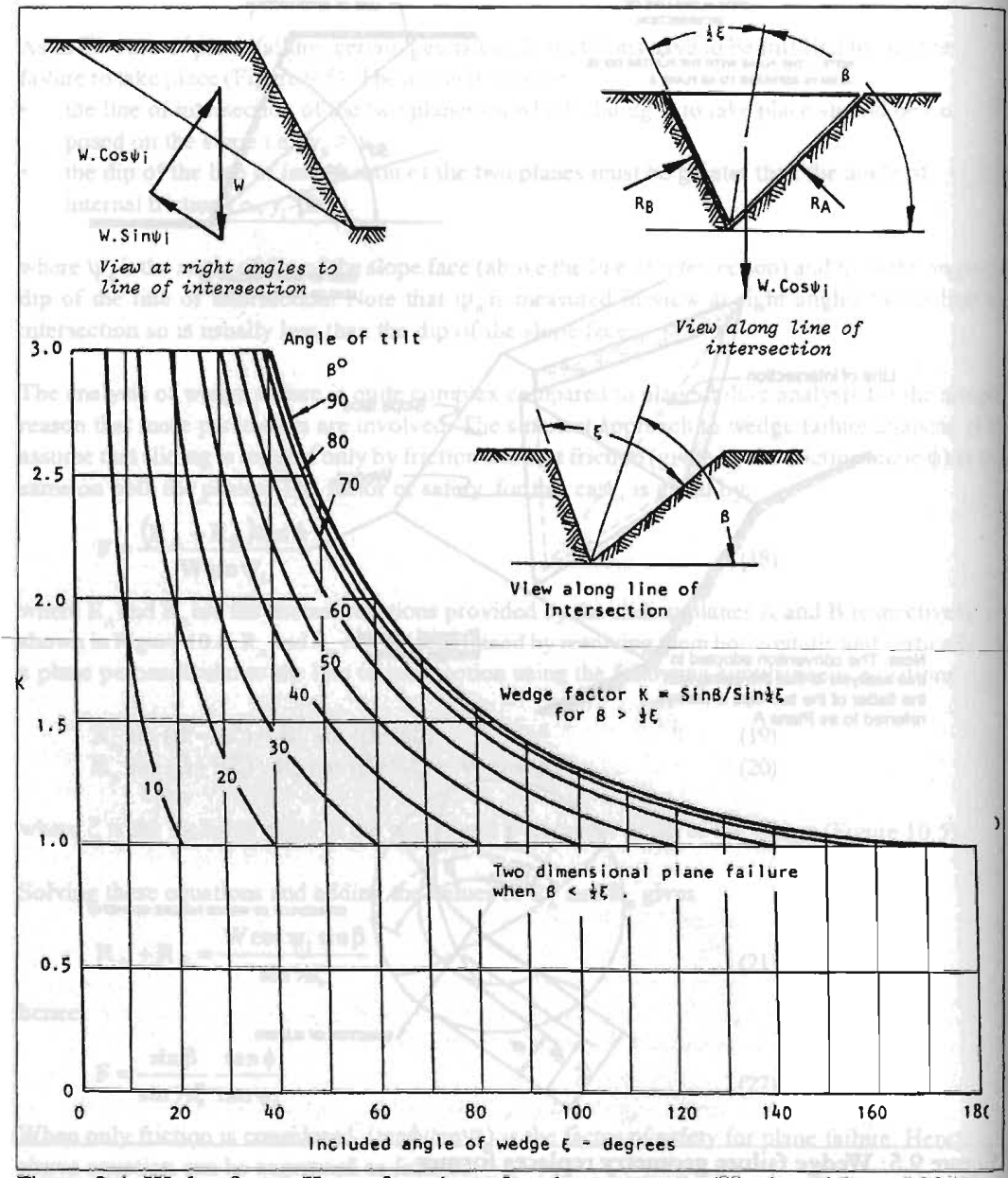

Figure 9.6: **Wedge factor K as a function of wedge geometry (Hoek and Bray 1981)**

Wedge analysis including cohesion and water pressure – 'full wedge analysis' – is based on the slope geometry shown in Figure 9.7. Note that

- the total height of the slope is the difference in vertical elevation between the levels where the line of intersection daylights on the slope below the crest and on the upper surface above the crest; and
- the water pressure distribution is based on the assumption that the wedge itself is impermeable and that water enters the top of the wedge along the traces 3 and 4 and leaves the slope along traces 1 and 2. The resulting water pressure distribution is shown in Figure 9.7; it is zero along lines 1, 2, 3, 4 and maximum along the line of intersection 5.

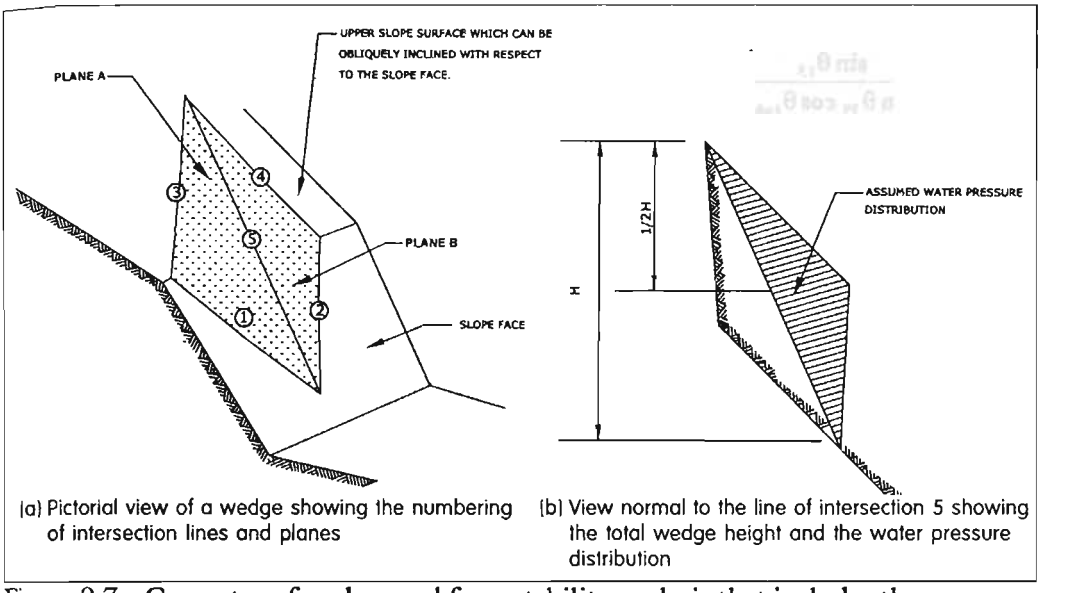

(a) Pictorial view of a wedge showing the numbering of intersection lines and planes

(b) View normal to the line of intersection 5 showing the total wedge height and the water pressure distribution

Figure 9.7: **Geometry of wedge used for a stability analysis that includes the influence of cohesion and water pressure on the failure surfaces** (after Hoek and Bray 1981)

Since these sorts of analyses are most effectively carried out using computers, it is of utmost importance to number the lines of intersection in the same sequence throughout. Following Hoek and Bray (1981) the numbering of the lines of intersection of various planes involved in wedge failure analysis (Figure 9.7a) is as follows:

1 - intersection of plane A with the slope face
2 - intersection of plane B with the slope face
3 - intersection of plane A with the upper slope surface
4 - intersection of plane B with the upper slope surface
5 - intersection of planes A and B

Now assuming that sliding always takes place along the line of intersection of the sliding surface numbered 5 above, the factor of safety is given by the following equation (Hoek and Bray 1981)

$$F = \frac{3}{\gamma H}\left(c_A X + c_B Y\right) + \left(A - \frac{\gamma_w}{2\gamma} X\right)\tan\phi_A + \left(B + \frac{\gamma_w}{2\gamma} Y\right)\tan\phi_B$$

where

c_A and c_B are the cohesive strengths of planes A and B

ϕ_A and ϕ_B are the angles of friction on planes A and B

γ and γ_w are the densities of rock and water

H is the total height of the wedge

X, Y, A and B are dimensionless factors which depend on the geometry of the wedge.

Thus

$$X = \frac{\sin\theta_{24}}{\sin\theta_{45}\cos\theta_{2na}}$$

$$Y = \frac{\sin\theta_{13}}{\sin\theta_{35}\cos\theta_{1nb}}$$

$$A = \frac{\cos\psi_a - \cos\psi_b\cos\theta_{na\,nb}}{\sin\psi_5\sin^2\theta_{na\,nb}}$$

$$B = \frac{\cos\psi_b - \cos\psi_a\cos\theta_{na\,nb}}{\sin\psi_5\sin^2\theta_{na\,nb}}$$

where ψ_a and ψ_b are the dips of planes A and B respectively and ψ_5 is the dip of the line of intersection 5.

Examples of the practical application of these analysis techniques are given in Part B.

Part B: Practical Examples of Rock Slope Stability Analysis

Example 1: Stability Analysis of Rock Slopes at the Dam Site of the Upper Arun Hydel Project

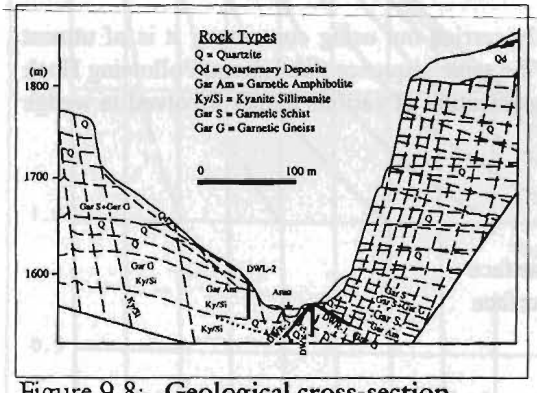

Figure 9.8: Geological cross-section 300m downstream of proposed Upper Arun dam site

Geological and geotechnical conditions at the dam site

The dam site of the Upper Arun Hydel Project is located in Sankhuwasabha in eastern Nepal. Stability analysis of the rock slope was carried out by the author. The site is underlain mainly by gneiss and quartzite rock. The right bank is very steep, it runs approximately parallel to the Arun river for about 380m and reaches a height of up to 240m above the river bed (Figure 9.8). The average slope of the cliff is approximately 70° to the horizontal at its lower levels up to 1700m elevation and 80° above this. The average strike of the cliff is N75E. The slope is intersected by a number of joints, bedding planes, foliation planes, and shear planes, al of which could affect the stability of the cliff and endanger the diversion structure. The discontinuities that are likely to govern the failure of the cliff are of four types.

Sub-vertical joints striking approximately NS (Joint set A) at orientations of

$270° \pm 10°/60 \pm 10°$ and $90° \pm 5°/80° \pm 10°$

Sub-vertical joints striking approximately EW (Joint set B) at orientations of

$180° \pm 10°/80 \pm 10°$ and $000° \pm 10°/85° \pm 5°$

Sub-horizontal foliation planes (Joint set C)

At the dam axis — lower part: 030° /20°; upper part: 180°/15°
Downstream of the dam: — lower part: 355°/ 20°; upper part: 040°/15°

Sub-horizontal shear planes (Joint set D)

320°/15°

The A-set joints are rather systematic. Some of the master joints, spaced at about 10 to 20m from each other, extend all along the cliff and beyond, with some up as far as Chepuwa village. In between there are a number of major joints spaced at about 5m, some of which extend up to the cliff top. Their depth into the cliff is estimated to be less than 3 to 5m, and they mostly terminate at the surface of the B-set joints.

The B-set joints are either stress relief or tension joints – mostly minor. It was not possible to measure their spacing; the estimated separation is about 10m.

The sub-horizontal C-set joints are either the bedding plane or foliation plane joints. Spacing between foliation planes in intact rock varies from 10 cm to a few metres; however, spacing between planes of weakness due to foliation or schistosity is estimated to be 10-20m. At this site, the foliation planes show greater scatter in terms of their dip direction and dip angle. The dipping is, in all cases, into the cliff. Figure 9.9 shows a stereographic plot of the various discontinuities.

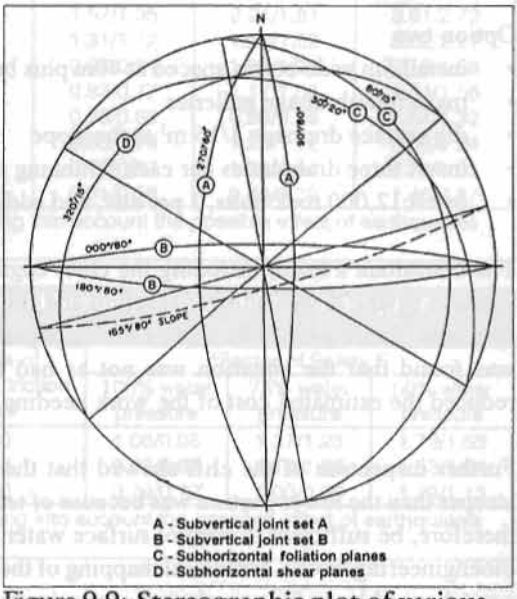

Figure 9.9: Stereographic plot of various discontinuities at the proposed Upper Arun dam site area

The upper surface of the slope is composed of quite thick residual/colluvial material that has a number of circular failures. A large one has been observed about 200m upslope. Seepage water emerges on the surface and there is a waterfall a few metres downstream of the dam site. This seepage water is, however, mainly in the middle portion of the slope; the two other ends of the slope (approximately northern and southern ends) are relatively well drained.

The left bank is also composed mainly of quartzite and gneiss but is comparatively massive. The lower part of the slope is flatter but the upper part is almost vertical and has, at places, slikensided

surfaces most probably due to fault movement. The portion above the flatter slope has a dense tree cover.

Stability analysis of the right cliff at the dam site of the Upper Arun Hydel Project

The left bank at the dam site was thought to be stable, but the World Bank Panel of Experts invited to assess the overall design of the project questioned the stability of the right bank. A consultant who had not visited the site previously carried out the analysis. To cover the worst case geological scenario for the engineering of the dam, the consultant postulated

- shear planes or planes of discontinuity may exist somewhere around the point where the cliffs become steeper at 1,700m where presumably the bedding planes also change their attitudes; and
- the reason for the upper portion of the slope being steeper than its lower portion may be that it is being pushed, albeit imperceptibly, by the overburden and other earth pressures.

The consultant suggested removing the overburden on the upper surface of the slope in addition to carrying out one of the following two options.

Option one

- install 5m wide berms spaced at 20m plus berm sealing and protection work
- dig surface drainage 1/50 m^2
- make 1900 drain holes

Option two

- install 5m wide berms spaced at 40m plus berm sealing and protection work
- make four drainage galleries
- dig surface drainage 1/15 m^2 at the slope
- insert three drain holes per each 5 running metres of gallery
- insert 12,000 rock bolts, 1 per 8m^2, and additional shotcrete

The consultant's team, including the chief engineer of the project, expressed concern about the solution saying it was an over-reaction and the previous field geologist had not expressed such concerns. Subsequently the author of this paper carried out a stability analysis of the slope and it was found that the situation was not as bad as postulated (see below). This finding greatly reduced the estimated cost of the work needing to be done.

Further inspection of the cliff showed that the reason for the upper portion of the slope being steeper than the lower portion was because of tectonic movement and not earth pressure. It would, therefore, be sufficient to control surface water on the upper surface of the slope by carrying out bioengineering works. Structural mapping of the slope showed that the rock mass was divided into a number of blocks by a number of approximately orthogonal joint sets. The cross-section shown in Figure 10.8 suggests that the most likely modes of failure are planar block sliding or planar block overturning.

Analysis of **planar block sliding** is equivalent to checking the safety of a retaining wall against base shear failure. The extent and spacing of various joints indicated that blocks of various sizes could be involved, with probable block sizes of 20m x 10m; 20m x 8m; 20m x 5m; 40m x m; and 40 m x 10 m. However, the size of the design block depends on its location on the slope face as shown in Tables 9.4, 9.5, 9.6, and 9.7.

Table 9.4: **Stability analysis of dam abutment area, upper half of the cliff (planar block sliding)**

Block size	Base angle a°	Back-face angle b°	Angle of internal friction (in degrees)	[a]Factor of safety F		
				100% water pressure	75% water pressure	50% water pressure
20 m x 10 m	0°	90°	40	2.09/1.80	2.93/2.41	4.61/3.48
			35	1.79/1.54	2.50/2.06	3.93/2.54
			30	1.52/1.32	2.13/1.75	3.33/1.82
	0°	80°	40	1.98/1.70	2.09/1.71	4.53/3.41
			35	1.69/1.45	1.78/1.47	3.87/2.91
			30	1.44/1.23	1.51/1.24	3.27/2.46
20 m x 8 m	0°	90°	40	1.68/1.48	2.35/2.00	3.69/2.93
			35	1.43/1.27	2.00/1.70	3.14/2.49
			30	1.21/1.07	1.70/1.44	2.66/2.11
	0°	80°	40	1.48/1.03	2.13/1.81	3.44/2.73
			35	1.25/1.11	1.87/1.54	2.91/2.30
			30	1.05/0.93	1.52/1.29	2.45/1.93
20 m x 5 m	0°	90°	40	1.05/0.98	1.47/1.32	2.30/1.98
			35	0.89/0.83	1.25/1.13	1.96/1.69
			30	0.76/0.70	1.06/0.96	1.66/1.43
	0°	80°	40	0.92/0.84	1.34/1.20	2.19/1.85
			35	0.78/0.72	1.15/1.04	1.87/1.58
			30	0.67/0.62	0.97/0.87	1.58/1.34
40 m x 20 m	0°	90°	40	1.97/1.69	2.76/2.27	4.36/3.29
			35	1.66/1.43	2.34/1.92	3.68/2.78
			30	1.39/1.19	1.95/1.60	3.08/2.33
	0°	80°	40	1.85/1.59	2.62/2.15	4.21/3.17
			35	1.57/1.35	2.21/1.81	3.61/2.72
			30	1.31/1.12	1.25/1.52	3.02/2.27
40 m x 10 m	0°	90°	40	0.98/0.91	1.38/1.24	2.18/1.88
			35	0.83/0.77	1.17/1.06	1.84/1.58
			30	0.70/0.65	0.98/0.88	1.54/1.32
	0°	80°	40	0.85/0.79	1.24/1.12	2.06/1.24
			35	0.72/0.67	1.04/0.94	1.74/1.05
			30	0.61/0.56	0.88/0.79	1.46/0.87

Note:[a]the second figure shows the factor of safety taking into account the possible effect of earthquakes (seismic coefficient)

Table 9.5: **Stability analysis of the eastern edge of the cliff facing Chepu Khola (planar block sliding)**

Block size	Base angle a°	Back-face angle b°	Angle of internal friction 0°	[a]Factor of Safety F		
				100% water pressure	75% water pressure	50% water pressure
20m x 10m	15° (away from the cliff)	90°	40	1.08/0.98	1.37/1.23	1.79/1.53
			35	0.93/0.84	1.18/1.06	1.53/1.34
			30	0.79/0.72	1.00/0.90	1.29/1.13

Note: [a]the second figure shows the factor of safety taking into account the possible effect of earthquakes (seismic coefficient)

Table 9.6: **Stability analysis of the slope downstream of diversion structure (planar block sliding)**

Block size	Base angle a°	Back-face angle b°	Angle of internal friction 0°	Factor of safely F		
				100% water pressure	75% water pressure	50% water pressure
20m x 10m	10° (into the cliff)	80°	40	2.53	3.51	5.48
			35	2.23	3.09	4.81
			30	1.97	2.71	4.22
		70°	40	2.43		5.42
			35	2.14		4.76
			30	1.89		4.18

Table 9.7: **Stability analysis of dam abutment area, upper half of the cliff (planar block overturning)**

Block size	Base angle a°	Slope angle b°	[a]Factor of safety F		
			100% water pressure	75% water pressure	50% water pressure
20m x 10m	0°	80°	1.54/1.35	2.03/1.73	3.08/2.42
	0°	70°	1.68/1.44	2.25/1.84	3.37/2.53
20m x 5m	0°	80°	0.67/0.61	1.15/.99	1.54/1.26
	0°	70°	0.93/0.85	1.24/1.10	1.86/1.57

Note: [a]the second figure shows the factor of safety taking into account the possible effect of earthquakes (seismic coefficient)

Calculations were performed for various block sizes and for 100%, 75%, and 50% hydrostatic water pressure. The results are presented in Tables 9.4, 9.5, 9.6, and 9.7. Note that the factors of safety as presented in these tables are smaller for smaller back face angles, which are also the slope angles. This is because friction along the back face of the block has not been considered.

The average dip angles were 20° and 15° respectively at the lower and higher elevations of the cliff. However, since the strike of the foliation plane was not parallel to that of the cliff, the base angle of the block will be smaller than the dip angle. In this analysis, the dip angles have been reduced conservatively by 40%. Other parameters assumed were

Density of rock: 2.7 t/m^3
Angle of internal friction: 40°/35°/30° to represent various possibilities.
Cohesion: c = 5 t/m^2

Analysis using **planar block overturning** sliding is equivalent to checking the safety of a retaining wall against overturning about its toe. The block dimensions and other parameters used here were the same as those assumed for planar block sliding.

Except for block sizes 20m x 5 m and 40m x 10m, for which the factor of safety was as low as 0.6 after considering the seismic coefficient suggested by the underground structure experts (0.06g), the slope was found to be stable. The factor of safety varied from about 1.30 for 100% saturation of rock having an angle of internal friction of 30° to over 3.0 for 50% saturated rocks. A few blocks at the upstream and downstream ends of the slope were found to be unstable; these will have to be removed as a part of the face trimming works.

Conclusions

The most probable block size has a base to height ratio of 1:2, but for the purpose of comparison blocks of base to height ratio of 1:2 to 1:4 were analysed. The angle of friction for this rock is likely to be more than 30° and the analysis shows that the cliff, except near its upstream and downstream faces, is probably stable. However, taking into consideration the magnitude and cost of the dam the following cliff stabilisation measures were suggested.

- Remove overhanging and/or loose rock pieces from the cliff
- Construct three rows of 2m x 2m, 200m long drainage galleries spaced at 50m vertical to 75m horizontal intervals
- Dig further drainage borings to connect these drainage galleries, some extending up to 50-75m into the rock; this should be done based on the observations of the drainage galleries
- Control surface water above the cliff and monitor the movement of the overburden and the cliff; the work associated with monitoring the movement of the overburden and the cliff should commence at least a year before the project starts

The analysis suggested that rock anchoring may not be required, but this can only be decided once the drainage galleries have been constructed and the deformation behaviour of the overburden above the cliff has been monitored.

If rock failure did occur it would start first at the northern and southern ends of the cliff where there is no confinement. It was therefore suggested that rock anchors be installed to tie at least two blocks at these ends at elevations of between 1,650m and 1,800m. Individual rock blocks along the top of the cliff may also need rock bolting.

Example 2: Stability Analysis of Rock Slopes at the Dam Site of the Kali Gandaki 'A' Hydel Project

Geological and geo-technical conditions at the dam site

The dam site of the Kali Gandaki 'A' Hydel Project is less than one kilometre downstream from the confluence of the Kali Gandaki River and the Andhi Khola. The desander basins of this project are planned to be placed on the left bank in highly fractured and crushed dolomite rock. This rock is also folded as shown by large variations in the dip direction of the bedding planes, which are intersected by closely spaced vertical to sub-vertical joints. The geological cross-section along the dam axis is shown in Figure 9.10.

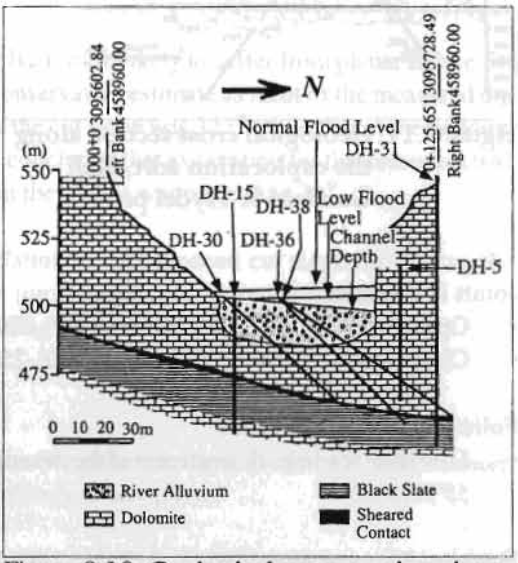

Figure 9.10: Geological cross-section along the dam axis of the Kali Gandaki 'A' hydel project (Kafle 1996)

The site is underlain by a 15-25m thick layer of black slate which is inclined at approximately 15° towards the river. A sub-vertical fault separates dolomite on the riverside from phyllites that extend deep into the slope. Contact between the two rock types was observed downstream of the desander basins and another about 200m upstream of the existing suspension bridge. The contact between the dolomite and overlying phyllite is not exposed on the surface. However, Kafle (1996) mentioned that the sheared, shattered, slickensided, closely jointed, and tightly folded carbonaceous phyllites found inside the adit (exploration tunnel) as well as in trenches and sections of core from different boreholes, provides evidence of some tectonic contact between the two rock types. Although it was not possible to exactly locate the position of the above-mentioned tectonic contact/fault inside the rock mass, its tentative position has been worked out extrapolated from the dip angle measured inside the adit (Figure 9.11).

The right bank of the Kali Gandaki just downstream of the dam site is less fractured than the left bank. It is vertical to overhanging and has stood stable for many years.

A considerable volume of excavation will have to be carried out for the construction of the intake structures and the desander basins. The height of excavation will reach to about 140m. The design proposes to line the lower portion of the cut slope adjacent to the desanders with concrete and

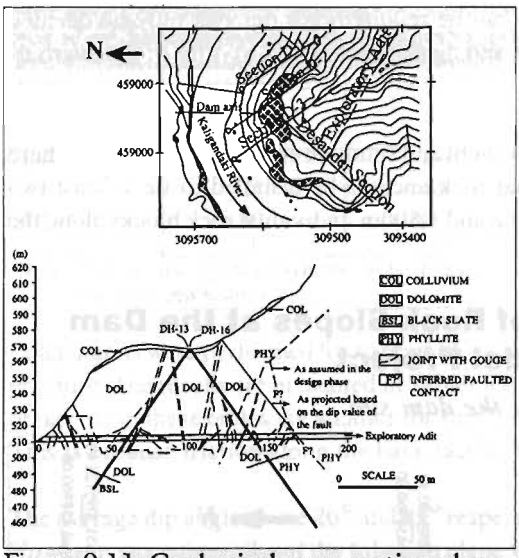

Figure 9.11: Geological cross section along the exploration adit, Kali Gandaki 'A' Hydel project

leave the remaining portion exposed. The upper portion of the slope is composed of highly and closely folded phyllites and schists and a cut slope could be designed as for soils. Since the desanders are to be placed in highly fractured and crushed dolomites, it is very important to analyse the stability of the cut slopes. Detailed structural mapping of the site has been carried out. The prominent structural features were found to be bedding planes, joints, and foliation planes.

Bedding planes (B1, B2 etc.) in dolomite

- B1 Series – low-level readings near the suspension bridge: 310°/15°, 305°/15°, 300°/10°
- B2 Series – mid-level readings on the exposed steep slope: 180°/10°, 185°/20°, 134°/50°, 195/30
- B3 Series – top-level readings near the top of the exposed slope in dolomite: 000°/45°

Joints in dolomite

- Open joints - 020°/80°, 045°/35°, 090°/70°, 050°/65°
- Closed joints - 350°/60°, 350°/65°,237°/70°, 250°/85°, 274°/35°, 042°/65°

Foliation planes in phyllites

- Low level readings downstream of the desanders: 130°/60°, 120°/35°, 295°/45°, 169°/60°, 162°/55°, 118°/35°/

Damsite - Mirmitar spur: 180°/45°, 312°/35°, 180°/40°, 168°/40°, 210°/20°

Cut slope: Approximately 322° (dip angle varies)

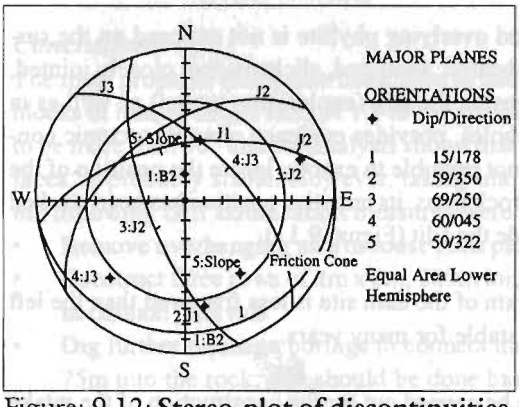

Figure: 9.12: Stereo-plot of discontinuities at the left bank of the Kali Gandaki 'A' dam site

Figure 9.12 shows a stereographic projection of the discontinuities and the cut slope. One field geologist suggested that data represented by the B1 series are of a local nature and that their attitudes (position relative to the horizontal) may have been changed by the combined effect of erosion, riverbank cutting, and the impact of large riverbed loads. Similarly, discontinuities represented by B3 series data are also thought to be of a local nature and they may not extend up to the excavation line. Hence this data was not considered for the analysis. The data selected as relevant for the stability analysis of rock slope and/or cut slopes in dolomite were

- joint sets J1, J2, and J3, and
- bedding plane B2

Stability analysis of cut slopes

In the initial design phase it was recognised that the cut slope at the upper part of the slope was composed of highly and closely folded phyllites and schists and so would be flatter. The upper part could be treated as if it was composed of soils. The lower part composed of dolomites could be cut at much steeper angles, depending of course on the measures to be taken to stabilise the cut slope. In the initial design phase, it was proposed bench the lower part of the slope with an average bench slope angle of 60°. Since this part of the slope was going to adjoin the desanding basins directly, however, the stability was more important. Although the slope was highly fractured, field observations indicated that the probable modes of failure were wedge failure and planar failure.

Of all the discontinuity surfaces, the bedding plane B2 is most likely to suffer from planar failure. Its average dip value is assumed to be 30°. This is a conservative estimate as most of the measured dip angle values are less than this. The dip direction of the cut slope was 322° while that of the bedding plane B2 varied between 134 and 195. Thus it was concluded that excavation for the desanders was unlikely to lead to plane failure as the difference in the strikes was more than 30°.

The three dimensional position of joint sets in relation to the proposed cut slope for placing the desanders showed that the following combination joints might lead to wedge failure

- Case A combination of joint set J1 and bedding plane
- Case B combination of joint sets J1 and J2
- Case C combination of joint sets J2 and J3.

Case A. The plunge of the line of intersection of the two planes is about 6° whereas the minimum friction angle is 30°. Therefore, wedge failure is unlikely to take place.

Case B. The dip value of the cut slope is greater than the plunge of the line of intersection of the two joint surfaces and the plunge is greater than the friction angle. Hence wedge failure is possible with the movement along the line of intersection. A detailed analysis is given in Table 10.8. The joint set J4 shown in the stereonet is not likely to be a problem as only a few of them were noted and they were not sufficiently persistent.

Case C. The two joint sets J2 and J3 are again likely to lead to wedge failure with sliding on both the surfaces. However, if the friction angle is assumed to be 35°, wedge failure is unlikely, thus case B is more critical.

Design of cut slopes in dolomite

Judging from a few boreholes and other visible surfacial lineations, the rock slope does not contain large through-going discontinuity surfaces but is highly jointed or fractured, thus wedge failures are most likely to be in the form of localised surface ravellings (rock breaking into small pieces). Analysis using stereographic projection suggested that such localised failures might take place if the slope were cut at angles steeper than about 50°.

Based on previous experience, the chief designer of the project chose a slope of 1:1 for the upper part which was composed of closely jointed and tightly folded carbonaceous phyllites, and an

average slope of 65° for the lower slopes, which are composed of dolomitic rocks with individual benches sloping at about 70°-73°.

The plan is to drain the slope by sub-surface drainage galleries so analysis was made assuming a dry state. The factor of safety was calculated to be 1.17 for a friction angle of 30° and 1.42 for a friction angle of 35°. Analysis using stereographic projection, however, showed that small scale localised ravellings could take place if the slope were cut at angles steeper than about 50°. Therefore localised patches will have to be stabilised by shotcreting, nailing, or bolting or a combination of these.

In view of the crucial importance of the stability of the cut slope, the initial design proposed was to line the lower part of the slope with concrete in addition to the treatments mentioned above. However, it was recognised that the actual position of the contact between dolomite and phyllite inside the slope as well as the position of the 15-25m thick layer of black slate below the riverbed would have to be taken into consideration. At the time of writing excavation of the desander basins was in progress and the tectonic contact between dolomite and the overlying phyllite had been found to be very complex. The design of the cut slope is therefore being revised.

The stereo plot of the relevant data with all the four planes and all the angles required are given in Figure 10.13. This figure also shows the stereographic method for calculating the angles required for wedge analysis. Computer software is also available to carry out such types of stability analysis.

Table 9.8: **Worked out example of wedge stability analysis of the cut slope behind the desander basins at Kali Gandaki 'A' Hydroelectric Project**

Discontinuity planes	dip°	dip direction°	properties
A (J1)	59	350	ϕ_A=35°,c_A=200kN/m²
B(J2)	69	250	ϕ_B=30°,c_B=200kN/m²
Slope surface	60	322	c= 200kN/m²
Upper surface	45	322	c=100kN/m²
Height H = 125m			

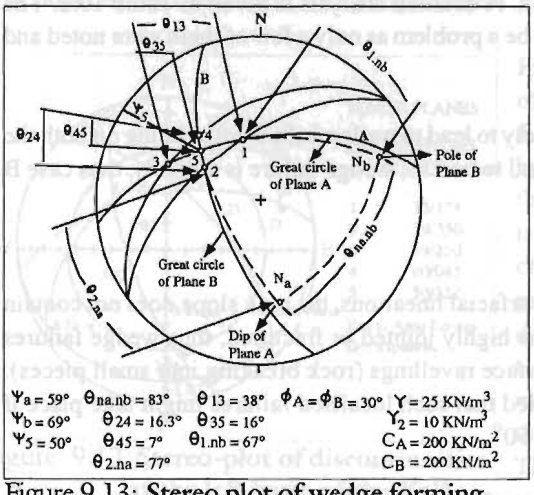

Figure 9.13: Stereo plot of wedge forming joints, Kali Gandaki 'A' Hydel project

Wedge stability calculation sheet

Of the various discontinuities mapped at the location of the desanding basins, joints J1 and J2 are those most likely to experience wedge failure. The input data related to these joints together with the assumed values of cohesion and friction are given above. Figure 10.13 shows a stereo plot of the wedge forming joints. The other details required for wedge stability analysis of the cut slope at the desanding basins are given in Table 9.9.

Note that the discontinuity parameters used for this example are only averaged values so localised failures may still occur. In rock slope stability analysis, it is not easy to make a reliable assessment of cohesion although this might affect the stability of the slope considerably. For example, if cohesion in the above example is reduced by 10%, the safety factor would be reduced to 1.5, generally considered to be the minimum acceptable, and if the cohesion were reduced by 17%, the corresponding safety factor would be only 1.3, the minimum value suggested by Hoek and Bray (1980).

Table 9.9: **Wedge stability calculation sheet for the cut-slope of the desanding basins, Kali Gandaki 'A' hydel project**

Input data	Function value	Calculation
$\psi_a = 59$ $\psi_b = 69°$ $\theta\psi_5 = 50°$ θna. Nb = 83°	Cos ψa = 0.515 Cos ψb = 0.358 Sin ψ5 = 0.766 Cos θna. Nb = 0.122 Sin θna. Nb = 0.992	$A = \frac{Cos\psi_a - Cos\psi_b.Cos\,\theta na \times nb}{Sin\psi_5 - Sin\,2\theta_{na} \times nb} = \frac{0.515 - 0.358x0.122}{0.766 \times 0.984} = 0.625$ $B = \frac{Cos\psi_b - Cos\psi_a.Cos\,\theta_{na} \times nb}{Sin\psi_5 - Sin\,2n_{na}\text{-}nb} = \frac{0.358\text{-}0.515x0.12}{0.766 \times 0.584} = 0.391$
θ 24 = 16.3° θ 45 = 7° θ 2.na = 77°	Sin θ 24 = 0.281 Sin θ45 = 0.122 Cos θ2.na = 0.225	$X = \frac{Sin\,\theta_{24}}{Sin\,\theta_{45}.Cos\,\theta_2.na} = \frac{0.281}{0.122 \times 0.225} = 10.237$
θ 13 = 38° θ 35 = 16° θ 1.nb = 67°	Sin θ 13 = 0.616 Sin θ 35 = 0.276 Cos θ 1.nb = 0.391	$Y = \frac{Sin\,\theta_{13}}{Sin\,\theta_{35}.Cos\,\theta_1.nb} = \frac{0.616}{0.276x0.391} = 5.708$
θ_A = 30° θ_B = 30° γ = 25KN/m³ γ_w = 10 KN/m³ CA = 200KN/m² CB = 200KN/m² H = 125m	tan θ_A = 0.577 tan θ_B = 0.577 $\frac{3\,C_A}{\gamma_H}$ = 0.192 $\frac{3C_B}{\gamma_H}$ = 0.192 $\frac{\gamma_w}{2\gamma}$ = 0.2	$F = \frac{3}{\gamma_H}(CA.X + CB.Y) + (A - \frac{\gamma_w}{2\gamma}X)\tan\theta_A + (B - \frac{\gamma_w}{2\gamma}Y)\tan\theta_B$ F = 0.192 x 10.237 + 0.192 x 5.708 - .820 - 0.433 = 1.81

Note: Since the draft of this paper was written some time back, construction work at the dam site has progressed considerably. Excavation and/or stabilisation of the left bank adjacent to the desanders is almost complete.

The lower part of the slope in dolomite has been cut at a slope of V:H 1:0.3, almost the same as proposed in the design phase. The final cut slope has been treated with 30 cm thick fibre reinforced shotcrete and up to 7 metre long rock bolts placed along a grid of 2m x 2m. The upper part of the slope composed of highly microfolded, thinly bedded, and foliated phyllites, however, proved very problematic. Initially this part of the slope was cut at a slope of 1:1, but was later flattened to a slope of 1.5:1 H:V due to its failure. It was shotcreted and further strengthened by up to 6m long rock dowels. However, it failed again, and as suggested by the World Bank Panel of Experts has now been flattened to a constant slope of 1.8:1. The final cut slope has been shotcreted, but no other reinforcing elements have been used.

Acknowledgements

I am thankful to The Institution of Mining and Metallurgy for giving permission to reproduce Figures 9.3, 9.4, 9.5, 9.6, 9.7 from the book Rock Slope Engineering by E. Hoek and J. Bray.

References

Barton, N.R. (1973) 'Review of A New Shear Strength Criterion for Rock Joints'. In *Eng. Geology*, 8, pp.287-332

Barton, N.R. (1997) 'The Shear Strength of Rock and Rock Joints'. In *Intl. J. Mech. Min. Sci. & Geomech. Abstr.* 13(10): 1-24

Blyth, F.G.H.; De Freitas, M.H. (1974) *Geology for Engineers* (6th Edition). London: Edward Arnold

Brown, E. T. (ed) (1981) *Rock Characterization Testing and Monitoring*, Oxford: Pergamon Press

Hoek, E.; Bray J. (1981) *Rock Slope Engineering.* London: Institute of Mining and Metallurgy

Hoek, E.; Kaiser, T.K.; Bawden, W.F. (1995) *Support of Underground Excavation in Hard Rock.* Netherlands: A. A. Balkema Rotterdam Brookfield

Kafle, K.N. (1996) 'Engineering Geological Study of the Kali Gandaki "A" Hydroelectric Project Area, Western Nepal Lesser Himalaya'. In *Jour. Nepal Geol. Soc.*, 13: 65-71

Price, N. J. (1966) *Fault and Joint Development in Brittle and Semi-brittle Rock.* Oxford: Pergamon Press

Wahlstrom, E.E. (1973) *Tunnelling in Rocks*. Amsterdam: Elsevier